Tumor Biol. (2011) 32:179–188
DOI 10.1007/s13277-010-0111-z

RESEARCH ARTICLE

MicroRNA-dependent regulation of PTEN after arsenic trioxide treatment in bladder cancer cell line T24

Yan Cao · Shi-Liang Yu · Yan Wang · Gui-Ying Guo · Qiang Ding · Rui-Hua An

Received: 25 June 2010 / Accepted: 9 September 2010 / Published online: 21 September 2010

Abstract Arsenic trioxide has shown remarkable biological activity against bladder cancer in some clinical studies. However, the mechanism of its action is unknown. Our aim was to find the relationship between miRNAs and arsenic trioxide treatment by using T24 human bladder carcinoma cells. By performing microRNA microarray and quantitative real-time PCR after ATO treatment, we found that expression levels of several miRNAs, in particular, miRNA-19a, were significantly decreased in T24 cell line. Furthermore, cell proliferation assay, flow cytometry analysis, prediction of miRNA targets, Western blot analysis, and luciferase reporter assay were performed to determine the role of mir-19a in affecting the biological behaviors of T24 cells. Several miRNAs were up-regulated or down-regulated in T24 cells treated with arsenic trioxide compared to their controls. If only changes above two folds were considered, two miRNAs were identified, miRNA-19a was down-regulated, while miRNA-222* was up-regulated. Among them, knockdown of miRNA-19a by anti-miRNA-19a transfection showed a positive therapeutic effect in bladder cancer cells by inhibiting cell growth and inducing cell apoptosis targeting PTEN through the PTEN/Akt pathway. Besides this, a synergy effect was detected between knockdown of miRNA-19a and arsenic trioxide. Arsenic trioxide altered miRNA expression profile in T24 cells. It seems miRNA-19a plays a critical role in the mechanism of arsenic trioxide treatment in bladder cancer. The synergy effect between miRNA-19a and arsenic trioxide that advocates targeting the mir-19a may represent a potential approach to enhance the efficacy and safety of ATO to treat bladder cancer by a decrease in dose.

Keywords Arsenic trioxide · T24 cells · MicroRNA · Apoptosis · PTEN

Introduction

Arsenic trioxide (ATO) has been used primarily in the treatment as a therapeutic agent for acute promyelocytic leukemia (APL) [1]. ATO was approved to treat relapsed APL by the US Food and Drug Administration (FDA) in 2000 [2]. It has been extensively investigated in neoplastic hematologic disorder and solid tumor such as prostate, kidney, cervix, bladder, neuroblastoma, glioma, and gastric cancer [3–6], owing to its various cytological effects including inhibition of angiogenesis, promotion of apoptosis, and growth inhibition. Proposed mechanisms for the apoptotic effects include induction of apoptosis through caspases activation, down-regulation of BCL-2, reactive oxygen species (ROS) [7–9], and interactions with multiple signaling pathways, including MAPK, P38, and AKT [10–13]. Although apoptosis or growth inhibition induced by ATO was reported in several solid tumor cell lines, it was not accepted clinically because of the reported chronic toxicities, carcinogenicity, and other side effects associated with the unachievable dose. Therefore, the molecular mechanisms of apoptosis induced by ATO were important to be clarified in addition with the enhancement and replacement ATO.

MicroRNAs (miRNA) are small nucleotide noncoding RNA molecules that function to control gene expression by binding with imperfect complementarity to the 3′

Yan Cao and Shi-Liang Yu are contributed equally to this work.

Y. Cao · S.-L. Yu · Y. Wang · G.-Y. Guo · Q. Ding · R.-H. An (✉)
Department of Urinary Surgery, The First Affiliated Hospital of Harbin Medical University,
23 Youzheng Street,
Harbin 150001 Heilongjiang, China
e-mail: anruihua_hayida@yahoo.cn

untranslated region (3′UTR) of the target mRNA. In recent studies, more and more miRNAs have shown their potential of being oncogene or anti-oncogene, which emerge in cell death, proliferation, tumorigenesis, differentiation, etc. [14–17] Several studies suggest that miRNAs may influence the chemotherapy effect of some cancer cells [18, 19].

In this study, we have shown the alteration of miRNA expression profile in bladder cancer cells after ATO treatment using miRNA microarrays. It suggests that specific miRNAs expression altered in bladder cancer cells after ATO treatment. The miRNA that most dramatically down-regulated was miR-19a, which might play a decisive role. Furthermore, we have showed the target genes of miR-19a might be involved in the mechanisms of ATO therapy.

Materials and methods

Cell lines The high-grade T24 human bladder carcinoma cells line was purchased from ATCC (Manassas, VA, USA) and was cultured following the manufacturer's instructions. The cells were grown in McCoy's 5A supplemented with 10% fetal bovine serum. McCoy's 5A and FCS were purchased from Hyclone (Logan, UT, USA).

RNA isolation Total RNAs were isolated using Trizol reagent (Invitrogen, Carlsbad, CA, USA) following the manufacturer's instructions for miRNA microarray or real-time PCR analysis.

miRNA microarray T24 cells were treated with 4 μM of ATO (Sigma, St. Louis, MO, USA) and incubated for 24 h, then, miRNA-enriched total RNA was extracted for miRNA microarray analysis. RNA of untreated T24 cells was extracted as control. miRNA microarray hybridization was performed by Beijing CapitalBio using fluorescein-labeled miRNAs, each miRNA microarray chip containing 1,320 probes, corresponding to 998 human (including 122 predicted miRNAs), 350 mouse, and 627 rat miRNAs found in the miRNA Registry (http://microrna.sanger.ac.uk/sequences/, miRBase12.0). SmartArray microarrayer (CapitalBio) was used for each probe, which was designed to be complementary to the full-length mature miRNA and printed in triplicate. Procedures were performed as described in detail (http://www.capitalbio.com); briefly, miRNAs were labeled using the T4 RNA ligase labeling method described by Thomson et al. before [20]. Arrays were scanned with a LuxScan 10 K-A double-channel laser scanner (CapitalBio), and images were analyzed using LuxScan 3.0 software (CapitalBio). Differentially expressed miRNAs were identified by Significance Analysis of Microarrays (SAM) software.

Quantitative real-time PCR for miRNA analysis RT-PCR quantification of mature miRNAs was conducted using TaqMan miRNAssays and following the manufacturer's supplied instructions (ABI, Foster City, CA, USA). Mean cycle threshold was determined in triplicate PCRs and U6 snRNA was used as the internal control.

miRNA transfection Mature miRNA and the miRNA negative control were purchased from GenePharma (Shanghai, China). miRNA mimics or miRNA inhibitor was transfected using Lipofectamine 2000 (Invitrogen) following the manufacturer's instructions. All transfections were carried out in triplicate. To transfect, we diluted miRNA mimics or miRNA inhibitor into 50 μl Opti-Mem into each well. Lipofectamine™ 2000 was mixed gently before use, then 1 μl was diluted in 50 μl Opti- MEM. This was mixed gently and incubated for 5 min at room temperature. After the 5-min incubation, the diluted oligomer was combined with the diluted Lipofectamine™ 2000. This was also mixed gently

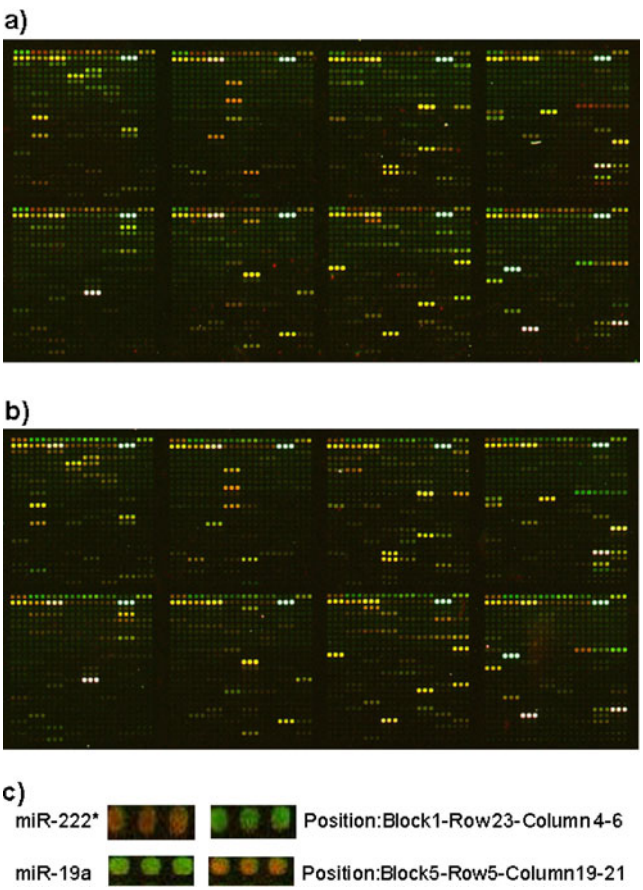

Fig. 1 miRNA expression profiling on miRNA microarray. **a** RNAs of the group treated with ATO were labeled with cy3 (*green*), and RNAs of the control group were labeled with cy5 (*red*). **b** As a dye-swap, RNAs of the group treated with ATO were labeled with cy5 (*red*), and RNAs of the control group were labeled with cy3 (*green*). **c** The four significant differentially expressed miRNAs

Table 1 Effect of ATO on miRNA expression in T24 cells

miRNA name	Fold change
hsa-miR-222*	3.83±0.12
hsa-miR-19a	0.49±0.08

and incubated for 20 min at room temperature. The oligomer-Lipofectamine™ 2000 complexes were added to each well containing 10,000 cells and medium. After 6 h, the medium was changed and the samples were assayed after 48 h.

Cell viability assay (CCK-8 assay) Cells (10,000 cells/well) were seeded in a 96-well plate, after a further 48 h transfection, 10 μM of CCK8 (Cell Counting Kit-8, Dojindo, Kumamoto, Japan) was added to each well and incubated for 2 h at 37°C. The OD_{450nm} was measured by a microplate reader (BMG LABTECH). All the experiments were performed in triplicate independently.

Flow cytometry analysis Detection of apoptotic cells after transfection was performed by using Annexin V/PI (Propidium Iodide) flow cytometric assay (BD Biosciences, San Jose, CA, USA) according to the manufacturer's instructions. In brief, transfected T24 cells were washed twice after being harvested with cold PBS and resuspended in100 μL cold Annexin V binding buffer (1×10^5 cells). After addition of 5 μL of Annexin V and 5 μL of PI, cells were incubated in the dark for 15 to 30 min at room temperature. Four hundred microliters of binding buffer was added per sample. Samples were analyzed using a FACSort flow cytometer (BD Biosciences). Values are given as means of three independent experiments.

Prediction of miRNA targets Potential miRNA targets were predicted and analyzed using miRecords [21] (http://mirecords.umn.edu/miRecords/), which contain 11 publicly available algorithms, including Pictar, miRanda, TargetScan, DIANA-microTest, Microinspector, miRDB, miTarget, NbmiRTar, PITA, RNA22, and RNAhybrid. To decrease the number of false-positive results, only putative target genes predicted by at least six programs were accepted.

Western blot analysis Forty-eight hours after miRNA transfection, T24 cells were lysed and protein was extracted. Western blot analysis was performed as described before [22]. Primary antibody of PTEN, Phospho-Akt, Akt (1:2,000 dilution) and β-actin (1:1,000 dilution) were purchased from Santa Cruz Biotechnology (Santa Cruz, CA, USA).

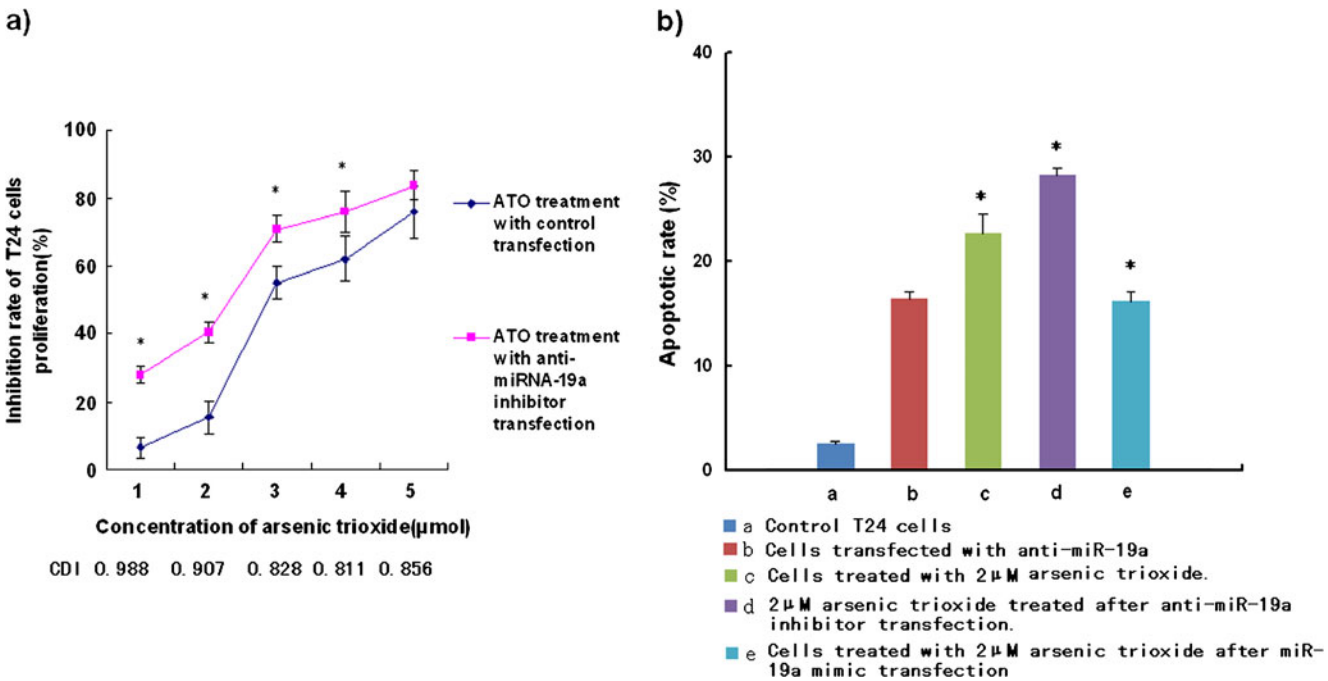

Fig. 2 **a** Comparison of ATO dose-dependent inhibition curves between cells transfected with anti-miR-19a inhibitor or control miRNA. Note that anti-miR-19a inhibitor transfection significantly enhanced the inhibition rate of ATO ($p<0.05$) at a low dose. The inhibition rate of T24 cells transfected with anti-miR-19a inhibitor is 24.2%. A synergy effect was detected between anti-miRNA-19a transfection and ATO treatment in T24 cells. All the experiments were performed in triplicate independently. **b** Determination of apoptosis of T24 cells after different treatment by flow cytometry. *a* Control T24 cells. *b* Cells transfected with anti-miR-19a. *c* Cells treated with 2 μM ATO. *d* Cells treated with 2 μM ATO after anti-miR-19a inhibitor transfection. *e* Cells treated with 2 μM ATO after miR-19a mimic transfection. Significant difference was found when *d* or *e* compared with *c* ($p<0.05$)

Table 2 Predicted target genes of miR-19a

Refseq	Symbol	Description
NM_000314	PTEN	Phosphatase and tensin homolog (mutated in multiple advanced cancers 1)
NM_014748	SNX17	Sorting nexin 17
NM_017974	ATG16L1	ATG16 autophagy related 16-like 1 (*Saccharomyces cerevisiae*)
NM_018043	TMEM16A	Transmembrane protein 16A
NM_018084	CCDC88A	Coiled-coil domain containing 88A
NM_018263	ASXL2	Additional sex combs like 2 (Drosophila)
NM_018900	PCDHA1	Protocadherin alpha 1
NM_018901	PCDHA10	Protocadherin alpha 10
NM_018905	PCDHA2	Protocadherin alpha 2
NM_018906	PCDHA3	Protocadherin alpha 3
NM_018907	PCDHA4	Protocadherin alpha 4
NM_018908	PCDHA5	Protocadherin alpha 5
NM_018909	PCDHA6	Protocadherin alpha 6
NM_018999	KIAA1128	KIAA1128
NM_019613	WDR45L	WDR45-like
NM_020168	PAK6	p21 protein (Cdc42/Rac)-activated kinase 6
NM_020182	PMEPA1	Prostate transmembrane protein, androgen induced 1
NM_017880	C2orf42	Chromosome 2 open reading frame 42
NM_017789	SEMA4C	Sema domain, immunoglobulin domain (Ig), transmembrane domain (TM) and short cytoplasmic domain, (semaphorin) 4C
NM_017786	GOLSYN	Golgi-localized protein
NM_014810	CEP350	Centrosomal protein 350 kDa
NM_014924	KIAA0831	KIAA0831
NM_014991	WDFY3	WD repeat and FYVE domain containing 3
NM_015017	USP33	Ubiquitin specific peptidase 33
NM_015049	TRAK2	Trafficking protein, kinesin binding 2
NM_015170	SULF1	Sulfatase 1
NM_015447	CAMSAP1	Calmodulin regulated spectrin-associated protein 1
NM_015955	MEMO1	Mediator of cell motility 1
NM_015995	KLF13	Kruppel-like factor 13
NM_016258	YTHDF2	YTH domain family, member 2
NM_016315	GULP1	GULP, engulfment adaptor PTB domain containing 1
NM_016472	C14orf129	Chromosome 14 open reading frame 129
NM_016530	RAB8B	RAB8B, member RAS oncogene family
NM_017610	RNF111	Ring finger protein 111
NM_017778	WHSC1L1	Wolf-Hirschhorn syndrome candidate 1-like 1
NM_020307	CCNL1	Cyclin L1
NM_020689	SLC24A3	Solute carrier family 24 (sodium/potassium/calcium exchanger), member 3
NM_020801	ARRDC3	Arrestin domain containing 3
NM_052897	MBD6	Methyl-CpG binding domain protein 6
NM_080836	STK35	Serine/threonine kinase 35
NM_138771	CCDC126	Coiled-coil domain containing 126
NM_139014	MAPK14	Mitogen-activated protein kinase 14
NM_144599	NIPA1	Non-imprinted in Prader-Willi/Angelman syndrome 1
NM_144720	JAKMIP1	Janus kinase and microtubule interacting protein 1
NM_144778	MBNL2	Muscleblind-like 2 (Drosophila)
NM_152271	LONRF1	LON peptidase N-terminal domain and ring finger 1
NM_152415	VPS37A	Vacuolar protein sorting 37 homolog A (*S. cerevisiae*)
NM_153690	FAM43A	Family with sequence similarity 43, member A
NM_153702	ELMOD2	ELMO/CED-12 domain containing 2

Table 2 (continued)

Refseq	Symbol	Description
NM_173582	PGM2L1	Phosphoglucomutase 2-like 1
NM_183376	ARRDC4	Arrestin domain containing 4
NM_198859	PRICKLE2	Prickle homolog 2 (Drosophila)
NM_206854	QKI	Quaking homolog, KH domain RNA binding (mouse)
NM_033225	CSMD1	CUB and Sushi multiple domains 1
NM_033211	C5orf30	Chromosome 5 open reading frame 30
NM_032961	PCDH10	Protocadherin 10
NM_020856	TSHZ3	Teashirt zinc finger homeobox 3
NM_021252	RAB18	RAB18, member RAS oncogene family
NM_021572	ENPP5	Ectonucleotide pyrophosphatase/phosphodiesterase 5 (putative function)
NM_022037	TIA1	TIA1 cytotoxic granule-associated RNA binding protein
NM_022080	NAPB	*N*-ethylmaleimide-sensitive factor attachment protein, beta
NM_022138	SMOC2	SPARC related modular calcium binding 2
NM_022374	ARL6IP2	ADP-ribosylation factor-like 6 interacting protein 2
NM_024490	ATP10A	ATPase, class V, type 10A
NM_024680	E2F8	E2F transcription factor 8
NM_024692	CLIP4	CAP-GLY domain containing linker protein family, member 4
NM_025187	C16orf70	Chromosome 16 open reading frame 70
NM_030962	SBF2	SET binding factor 2
NM_032039	ITFG3	Integrin alpha FG-GAP repeat containing 3
NM_032160	DSEL	Dermatan sulfate epimerase-like
NM_032505	KBTBD8	Kelch repeat and BTB (POZ) domain containing 8
NM_207371	C10orf140	Chromosome 10 open reading frame 140
NM_014382	ATP2C1	ATPase, Ca++ transporting, type 2C, member 1
NM_000125	ESR1	Estrogen receptor 1
NM_002233	KCNA4	Potassium voltage-gated channel, shaker-related subfamily, member 4
NM_002267	KPNA3	Karyopherin alpha 3 (importin alpha 4)
NM_002518	NPAS2	Neuronal PAS domain protein 2
NM_002841	PTPRG	Protein tyrosine phosphatase, receptor type, G
NM_002880	RAF1	v-raf-1 murine leukemia viral oncogene homolog 1
NM_002897	RBMS1	RNA binding motif, single stranded interacting protein 1
NM_002956	CLIP1	CAP-GLY domain containing linker protein 1
NM_003070	SMARCA2	SWI/SNF related, matrix associated, actin dependent regulator of chromatin, subfamily a, member 2
NM_003107	SOX4	SRY (sex determining region Y)-box 4
NM_003185	TAF4	TAF4 RNA polymerase II, TATA box binding protein (TBP)-associated factor, 135 kDa
NM_003244	TGIF1	TGFB-induced factor homeobox 1
NM_003245	TGM3	Transglutaminase 3 (E polypeptide, Protein-glutamine-gamma-glutamyltransferase)
NM_003272	GPR137B	G protein-coupled receptor 137B
NM_003629	PIK3R3	Phosphoinositide-3-kinase, regulatory subunit 3 (gamma)
NM_003654	CHST1	Carbohydrate (keratan sulfate Gal-6) sulfotransferase 1
NM_002222	ITPR1	Inositol 1,4,5-triphosphate receptor, type 1
NM_002024	FMR1	Fragile X mental retardation 1
NM_001759	CCND2	Cyclin D2
NM_000165	GJA1	Gap junction protein, alpha 1, 43 kDa
NM_000332	ATXN1	Ataxin 1
NM_000891	KCNJ2	Potassium inwardly-rectifying channel, subfamily J, member 2
NM_001001928	PPARA	Peroxisome proliferator-activated receptor alpha
NM_001002243	AFTPH	Aftiphilin

Table 2 (continued)

Refseq	Symbol	Description
NM_001002860	BTBD7	BTB (POZ) domain containing 7
NM_001083	PDE5A	Phosphodiesterase 5A, cGMP-specific
NM_001092	ABR	Active BCR-related gene
NM_001156	ANXA7	Annexin A7
NM_001204	BMPR2	Bone morphogenetic protein receptor, type II (serine/threonine kinase)
NM_001304	CPD	Carboxypeptidase D
NM_001390	DTNA	Dystrobrevin, alpha
NM_001452	FOXF2	Forkhead box F2
NM_001584	MPPED2	Metallophosphoesterase domain containing 2
NM_001693	ATP6V1B2	ATPase, H + transporting, lysosomal 56/58 kDa, V1 subunit B2
NM_003896	ST3GAL5	ST3 beta-galactoside alpha-2,3-sialyltransferase 5
NM_003955	SOCS3	Suppressor of cytokine signaling 3
NM_003972	BTAF1	BTAF1 RNA polymerase II, B-TFIID transcription factor-associated, 170 kDa (Mot1 homolog, *S. cerevisiae*)
NM_006251	PRKAA1	Protein kinase, AMP-activated, alpha 1 catalytic subunit
NM_006352	ZNF238	Zinc finger protein 238
NM_006421	ARFGEF1	ADP-ribosylation factor guanine nucleotide-exchange factor 1 (brefeldin A-inhibited)
NM_006464	TGOLN2	Trans-golgi network protein 2
NM_006469	IVNS1ABP	Influenza virus NS1A binding protein
NM_006526	ZNF217	Zinc finger protein 217
NM_006544	EXOC5	Exocyst complex component 5
NM_006624	ZMYND11	Zinc finger, MYND domain containing 11
NM_006813	PNRC1	Proline-rich nuclear receptor coactivator 1
NM_007023	RAPGEF4	Rap guanine nucleotide exchange factor (GEF) 4
NM_007054	KIF3A	Kinesin family member 3A
NM_007106	UBL3	Ubiquitin-like 3
NM_012081	ELL2	Elongation factor, RNA polymerase II, 2
NM_012342	BAMBI	BMP and activin membrane-bound inhibitor homolog (*Xenopus laevis*)
NM_013433	TNPO2	Transportin 2 (importin 3, karyopherin beta 2b)
NM_006246	PPP2R5E	Protein phosphatase 2, regulatory subunit B", epsilon isoform
NM_005935	AFF1	AF4/FMR2 family, member 1
NM_005639	SYT1	Synaptotagmin I
NM_004040	RHOB	Ras homolog gene family, member B
NM_004293	GDA	Guanine deaminase
NM_004299	ABCB7	ATP-binding cassette, sub-family B (MDR/TAP), member 7
NM_004458	ACSL4	Acyl-CoA synthetase long-chain family member 4
NM_004505	USP6	Ubiquitin specific peptidase 6 (Tre-2 oncogene)
NM_004525	LRP2	Low-density lipoprotein-related protein 2
NM_004571	PKNOX1	PBX/knotted 1 homeobox 1
NM_004859	CLTC	Clathrin, heavy chain (Hc)
NM_004869	VPS4B	Vacuolar protein sorting 4 homolog B (*S. cerevisiae*)
NM_004992	MECP2	Methyl CpG binding protein 2 (Rett syndrome)
NM_005112	WDR1	WD repeat domain 1
NM_005178	BCL3	B-cell CLL/lymphoma 3
NM_005230	ELK3	ELK3, ETS-domain protein (SRF accessory protein 2)
NM_005502	ABCA1	ATP-binding cassette, sub-family A (ABC1), member 1
NM_005578	LPP	LIM domain containing preferred translocation partner in lipoma
NM_014372	RNF11	Ring finger protein 11

Luciferase reporter assay For luciferase assays, pGL3 Firefly Luciferase reporter vector (Promega, Madison, WI, USA) was transfected into T24 cells with the 3′UTR fragment of human *PTEN* cDNA containing the putative target site for miR-19a. Renilla luciferase construct was co-transfected considering normalization of transfection efficiency. Twenty-four hours post transfection, dual-luciferase assay (Promega) was carried out as described by the manufacturer. Relative firefly luciferase activity of the samples was normalized against the value of Renilla luciferase activity. Experiments were performed more than three times independently.

Statistical analysis Data were expressed as means ± SD and compared via Student's *t* test for paired samples. Statistical significance was accepted at $P<0.05$.

Results

Altered expression of miRNAs in T24 cells with ATO treatment

The relative Cy3 and Cy5 dye intensity levels are shown in Fig. 1. SAM software using miRNA microarray data revealed that 30 miRNAs were upregulated and 49 were down-regulated after ATO treatment compared with untreated controls. If only significant differential expressed miRNAs (greater than twofold difference) were considered, two miRNAs were identified; among them, miR-222* was up-regulated and miR-19a was down-regulated after ATO treatment (Table 1).

The expression of mature miRNA-222* and miRNA-19a was confirmed by real-time PCR

To confirm the differential expression of miRNAs after ATO treatment (greater than twofold difference), the expressions of mature miRNA-222* and miRNA-19a were examined by qRT-PCR. Consistent with microarray results, the expression of miRNA-222* was up-regulated and miR-19a was down-regulated significantly with ATO treatment compared with untreated control samples (hsa-miR-222*: 2.32±0.24; hsa-miR-19a: 0.42±0.25) (Fig. 3b).

Anti-miRNA-19a inhibited T24 cells proliferation

To investigate whether the two miRNAs contribute to cell viability, T24 cells were transfected with miRNA-222* mimic and anti-miRNA-19a, respectively, for 48 h. The cck8-based cell viability assay demonstrated anti-miRNA-19a obtained an inhibition rate above 20% (24.2%), while miRNA-222* mimic obtained 6.9%. Based on these results, we focus on miRNA-19a for our further studies. Interestingly, a synergy effect was detected when anti-miRNA-19a was transfected into T24 cells with ATO treatment, which may lead to equal efficacy and lower dose of ATO treatment (Fig. 2a). CDI is calculated according to the formula $CDI = AB/(A*B)$, where AB is the ratio of cell viability index of the combination group of ATO treatment and anti-miR-19a inhibitor transfection to the control group and *A* or *B* is the ratio of viability index of the single agent groups to the control group. A value of CDI less than, equal

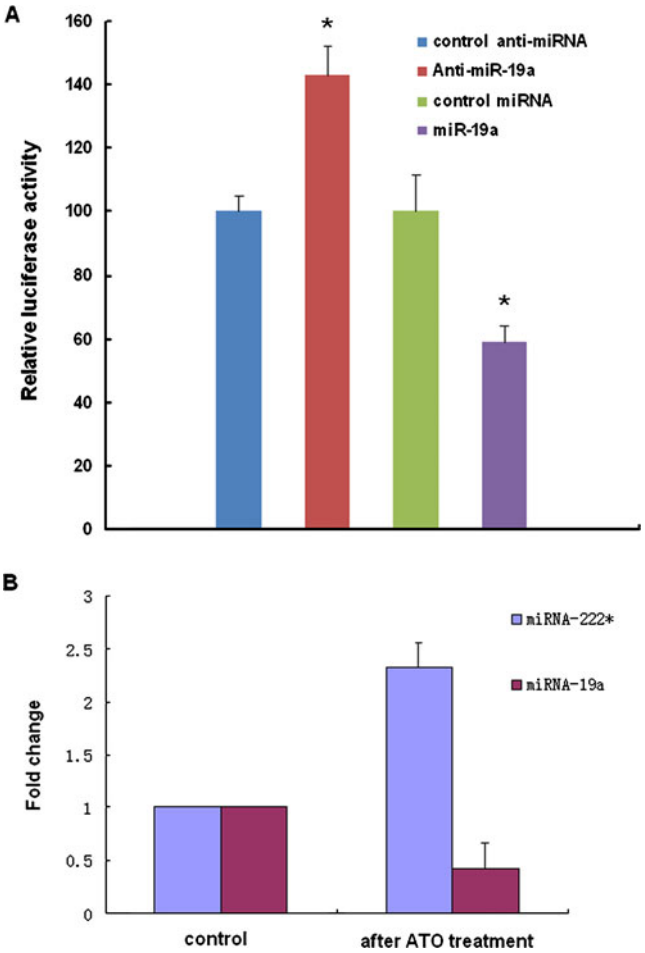

Fig. 3 **a** Luciferase activity assay. T24 cells were co-transfected with the luciferase reporter vector, which contained PTEN 3′-UTR fragment, and miR-19a, anti-miR-19, or control sequence. Luciferase activity was measured to determine the effect of these miRNAs on luciferase translation. Firefly luciferase activity of cells was assayed 48 h after transfection and renilla luciferase was used as transfection efficiency correction. Negative control was set as 100%. PTEN 3′-UTR-luciferase activity was decreased significantly in T24 cells transfected with miR-19a mimic, while silencing miR-19a with anti-miR-19a inhibitor led to a higher luciferase activity in T24 cells ($p<0.05$). **b** RT-PCR: the expression of miRNA-222* was up-regulated and miR-19a was down-regulated significantly with ATO treatment compared with untreated control samples (hsa-miR-222*: 2.32±0.24; hsa-miR-19a: 0.42±0.25)

to, or greater than 1 indicates that the drugs are synergistic, additive, or antagonistic, respectively.

Apoptosis mediated by miR-19a

In our study, transfection of anti-miRNA-19a into T24 cells was found to induce cell apoptosis; furthermore, transfection with anti-miR-19a inhibitor enhanced the apoptosis effects induced by ATO, while the apoptosis effect of ATO attenuated by miR-19a mimic transfection on T24 cells ($p<0.05$) (Fig. 2b).

Target gene prediction of miR-29a

We used the united prediction algorithm miRecords to identify targets of miR-19a and found most promising 143 candidate genes (Table 2), which is predicted by six databases, except *PTEN*, which is predicted by seven databases. Then, *PTEN* was chosen for further studies because it is a well-known tumor suppressor gene associated with many kinds of cancers and apoptosis pathways; more importantly, it has been proven to be involved in ATO treatment.

PTEN is a direct target of miR-19a

The results showed a significant decrease in luciferase activity for the 3′UTR of PTEN transfected with miR-19a mimic compared with the control, whereas the 3′UTR luciferase showed much higher activity when transfected with miR-19a inhibitor in T24 cells ($p<0.05$) (Fig. 3a). Therefore, miR-19a represses *PTEN* by binding to the 3′ UTR of *PTEN* in a direct manner at the posttranscriptional level.

Anti-miRNA-19a promotes protein PTEN

PTEN protein expression was significantly decreased in T24 cells transfected with miRNA-19a, while transfection of anti-miRNA-19a led to increased expression of PTEN protein in T24 cells. ATO treatment increased PTEN protein expression, while transfection with the miR-19a suppressed the function of ATO. These results indicate that miRNA-19a may play a crucial role in ATO treatment and PTEN regulation (Fig. 4).

Discussion

miRNAs represent a class of small non-protein coding regulatory RNAs that have central roles in gene silencing and function as oncogenes or tumor suppressors. miRNAs were also found to be potentially useful for therapeutic purposes recently [23, 24]. ATO has been effectively used for many years to treat patients with cancers due to its remarkable biological effects on several cellular functions, including growth-inhibitory and proapoptotic effects. Previous data from our laboratory show that activation of

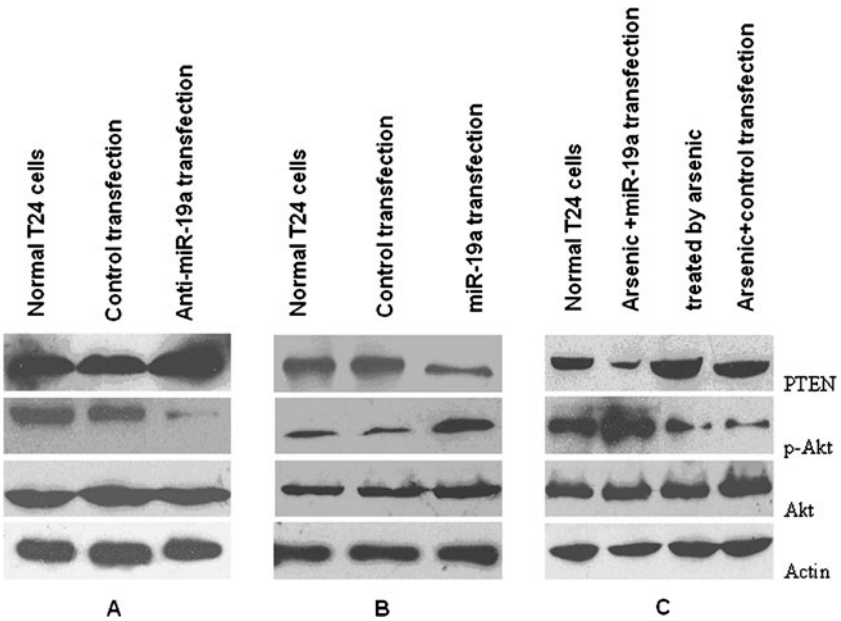

Fig. 4 Western blot analysis. **a** Transfection with the anti-miR-19a inhibitor increased the PTEN expression and induced a significant decrease in P-AKT (phosphorylation levels of Akt) protein expression in T24 cells. **b** Overexpression of miR-19a induced a significant decrease in PTEN protein expression and increased the P-AKT expression. **c** Arsenic increased the PTEN protein expression in T24 cells, while transfection with miR-29a counteracted ATO function

several signaling pathways mediates the arsenic-induced apoptotic signal in T24 cells [22]. As miRNAs have been considered to be interacted with many well-recognized cell signal pathways, we hypothesized that ATO would alter the expression profile of miRNAs in human bladder cancer cells, which may reveal the role of miRNAs in ATO treatment.

The microarray analysis identified 67 miRNAs that were up- or down-regulated in T24 cells following ATO treatment. Among them, two miRNAs (miR-19a, miR-222*) were selected according to the twofold criterion. Furthermore, anti-miR-19a showed a strong inhibition of cell proliferation of T24 cells and an increased apoptotic rate compared with control after transfection. Unexpectedly, miR-222* transfection did not show clear positive results. These results indicate that miR-19a is the most potent growth suppressor or apoptosis inducer in the ATO treatment of T24 cells. Interestingly, we showed that ATO gets a satisfactory growth inhibition and apoptotic rate at a low dose of 1.0 μmol/L with transfection of anti-miR-19a. This result could effectively improve the clinical utility of ATO treatment for its lower dose, which, in turn, lowered toxic side effects.

miR-19a belong to the miR-17–92 cluster, which is localized on chromosome 13q31.3 and is well known for its oncogenic role as reported [25–27]. In our study, we performed miR-19a overexpression and depletion in bladder cancer T24 cells and observed an obvious change in cell growth and apoptosis in this cell line. Indeed, we showed that transfection of T24 cells with anti-miR-19a resulted in decreased cell viability and induction of cell death. For further study, we focus on the targets of miR-19a because miRNAs exert their function through translational repression or degradation of mRNA targets. To predict the target genes of miR-19a, we used miRecords and finally chose *PTEN* for further studies as *PTEN* was a well-known anti-oncogene and has been confirmed to be involved in ATO treatment before [28]. Western blot results showed that over-expression of miR-19a decreased the expression of PTEN and depletion of miR-19a increased the expression of protein PTEN by analysis (Fig. 4). Furthermore, the phosphorylation levels of Akt, a major target of PTEN, increased by over-expression of miR-19a and decreased by depletion of miR-19a. Our luciferase reporter assays also confirmed that *PTEN* was a direct target for miR-19a in bladder cancer T24 cells as reported before in other cell lines [29]. ATO has been proved previously to upregulate the expression of PTEN [28], which coincided with our results that the expression of PTEN was increased in T24 cells treated with ATO. We reported that ATO treatment of T24 cells decreased the expression of miR-19a and also up-regulated the expression of its target gene *PTEN* with increased expression of protein PTEN and decreased expression of protein phospho-Akt, and the miR-19a mimics suppressed the effect of ATO on *PTEN*. The results indicate that miR-19a–PTEN–Akt was one of the important pathways of ATO on cancer cells.

Our study is the first to examine miRNAs expression alteration in human bladder cancer cells after ATO treatment. Whether the differential expressed miRNAs influence other biological activity against bladder cancer or in vivo remains to be investigated in future studies. However, our data provide evidence that miRNAs could serve as a potential approach to enhance the efficacy and safety of ATO treatment. We were overwhelmed to see the synergy effect between anti-miR-19a and ATO for its further clinical usefulness.

Conflict of interest statement None declared

References

1. Shen ZX, Chen GQ, Ni JH, et al. Use of arsenic trioxide (As2O3) in the treatment of acute promyelocytic leukemia (APL): II. Clinical efficacy and pharmacokinetics in relapsed patients. Blood. 1997;89:3354–60.
2. Soignet SL, Frankel SR, Douer D, et al. United States multicenter study of arsenic trioxide in relapsed acute promyelocytic leukemia. J Clin Oncol. 2001;19:3852–60.
3. Chen X, Zhang M, Liu LX. The overexpression of multidrug resistance-associated proteins and gankyrin contribute to arsenic trioxide resistance in liver and gastric cancer cells. Oncol Rep. 2009;22:73–80.
4. Karlsson J, Pietras A, Beckman S, Pettersson HM, Larsson C, Pahlman S. Arsenic trioxide-induced neuroblastoma cell death is accompanied by proteolytic activation of nuclear Bax. Oncogene. 2007;26:6150–9.
5. Lin TH, Kuo HC, Chou FP, Lu FJ. Berberine enhances inhibition of glioma tumor cell migration and invasiveness mediated by arsenic trioxide. BMC Cancer. 2008;8:58.
6. Murgo AJ. Clinical trials of arsenic trioxide in hematologic and solid tumors: overview of the National Cancer Institute Cooperative Research and Development Studies. Oncologist. 2001;6 Suppl 2:22–8.
7. Bi X, Gu J, Guo Z, et al. Different pathways are involved in arsenic-trioxide-induced cell proliferation and growth inhibition in human keratinocytes. Skin Pharmacol Physiol. 2010;23:68–78.
8. Cai BZ, Meng FY, Zhu SL, et al. Arsenic trioxide induces the apoptosis in bone marrow mesenchymal stem cells by intracellular calcium signal and caspase-3 pathways. Toxicol Lett. 2010;193:173–8.
9. Han YH, Moon HJ, You BR, Kim SZ, Kim SH, Park WH. Effects of arsenic trioxide on cell death, reactive oxygen species and glutathione levels in different cell types. Int J Mol Med. 2010;25:121–8.
10. Han YH, Moon HJ, You BR, Kim SZ, Kim SH, Park WH. The effect of MAPK inhibitors on arsenic trioxide-treated Calu-6 lung cells in relation to cell death, ROS and GSH levels. Anticancer Res. 2009;29:3837–44.
11. Mandegary A, Hosseini R, Ghaffari SH, et al. The expression of p38, ERK1 and Bax proteins has increased during the treatment of

newly diagnosed acute promyelocytic leukemia with arsenic trioxide. Ann Oncol. 2010;21:1884–90.
12. Mann KK, Colombo M, Miller Jr WH. Arsenic trioxide decreases AKT protein in a caspase-dependent manner. Mol Cancer Ther. 2008;7:1680–7.
13. Wen J, Feng Y, Huang W, et al. Enhanced antimyeloma cytotoxicity by the combination of arsenic trioxide and bortezomib is further potentiated by p38 MAPK inhibition. Leuk Res. 2010;34:85–92.
14. Friedland DR, Eernisse R, Erbe C, Gupta N, Cioffi JA. Cholesteatoma growth and proliferation: posttranscriptional regulation by microRNA-21. Otol Neurotol. 2009;30:998–1005.
15. Guo L, Ding ZH. Advances in the studies of miRNAs and cell apoptosis. Sheng Li Ke Xue Jin Zhan. 2007;38:331–5.
16. Li Y, Guessous F, Zhang Y, et al. MicroRNA-34a inhibits glioblastoma growth by targeting multiple oncogenes. Cancer Res. 2009;69:7569–76.
17. Vecchione A, Croce CM. Apoptomirs: small molecules have gained the license to kill. Endocr Relat Cancer. 2010;17:F37–50.
18. Ren Y, Zhou X, Mei M, et al. MicroRNA-21 inhibitor sensitizes human glioblastoma cells U251 (PTEN-mutant) and LN229 (PTEN-wild type) to taxol. BMC Cancer. 2010;10:27.
19. Zhong M, Ma X, Sun C, Chen L. MicroRNAs reduce tumor growth and contribute to enhance cytotoxicity induced by gefitinib in non-small cell lung cancer. Chem Biol Interact. 2010;184:431–8.
20. Thomson JM, Parker J, Perou CM, Hammond SM. A custom microarray platform for analysis of microRNA gene expression. Nat Methods. 2004;1:47–53.
21. Xiao F, Zuo Z, Cai G, Kang S, Gao X, Li T. miRecords: an integrated resource for microRNA-target interactions. Nucleic Acids Res. 2009;37:D105–110.
22. Wang Y, An R, Dong X, Pan S, Duan G, Sun X. Protein kinase C is involved in arsenic trioxide-induced apoptosis and inhibition of proliferation in human bladder cancer cells. Urol Int. 2009; 82:214–21.
23. Akao Y, Nakagawa Y, Hirata I, et al. Role of anti-oncomirs miR-143 and -145 in human colorectal tumors. Cancer Gene Ther. 2010;17:398–408.
24. Li Y, Kong D, Wang Z, Sarkar FH. Regulation of microRNAs by Natural Agents: an emerging field in chemoprevention and chemotherapy research. Pharm Res. 2010;27:1027–41.
25. Doebele C, Bonauer A, Fischer A, et al. Members of the microRNA-17-92 cluster exhibit a cell intrinsic anti-angiogenic function in endothelial cells. Blood. 2010;115:4631–3.
26. Loven J, Zinin N, Wahlstrom T, et al. MYCN-regulated microRNAs repress estrogen receptor-alpha (ESR1) expression and neuronal differentiation in human neuroblastoma. Proc Natl Acad Sci U S A. 2010;107:1553–8.
27. Pezzolesi MG, Platzer P, Waite KA, Eng C. Differential expression of PTEN-targeting microRNAs miR-19a and miR-21 in Cowden syndrome. Am J Hum Genet. 2008;82:1141–9.
28. Wang R, Li H, Guo G, et al. Augmentation by carnosic acid of apoptosis in human leukaemia cells induced by arsenic trioxide via upregulation of the tumour suppressor PTEN. J Int Med Res. 2008;36:682–90.
29. Lewis BP, Shih IH, Jones-Rhoades MW, Bartel DP, Burge CB. Prediction of mammalian microRNA targets. Cell. 2003;115:787–98.